

Proceedings of the Institution of Mechanical Engineers, Part D: Journal of Automobile Engineering

<http://pid.sagepub.com/>

Investigation of turbocharged diesel engine operation, exhaust emissions, and combustion noise radiation during starting under cold, warm, and hot conditions

C D Rakopoulos, A M Dimaratos and E G Giakoumis

Proceedings of the Institution of Mechanical Engineers, Part D: Journal of Automobile Engineering 2011 225: 1118

originally published online 20 June 2011

DOI: 10.1177/0954407011400155

The online version of this article can be found at:

<http://pid.sagepub.com/content/225/9/1118>

Published by:



<http://www.sagepublications.com>

On behalf of:



[Institution of Mechanical Engineers](http://www.imechE.org)

Additional services and information for *Proceedings of the Institution of Mechanical Engineers, Part D: Journal of Automobile Engineering* can be found at:

Email Alerts: <http://pid.sagepub.com/cgi/alerts>

Subscriptions: <http://pid.sagepub.com/subscriptions>

Reprints: <http://www.sagepub.com/journalsReprints.nav>

Permissions: <http://www.sagepub.com/journalsPermissions.nav>

Citations: <http://pid.sagepub.com/content/225/9/1118.refs.html>

Investigation of turbocharged diesel engine operation, exhaust emissions, and combustion noise radiation during starting under cold, warm, and hot conditions

C D Rakopoulos*, A M Dimaratos, and E G Giakoumis

Internal Combustion Engines Laboratory, Thermal Engineering Department, School of Mechanical Engineering, National Technical University of Athens, Athens, Greece

The manuscript was received on 14 September 2010 and was accepted after revision for publication on 21 January 2011.

DOI: 10.1177/0954407011400155

Abstract: Control of performance and transient emissions from turbocharged diesel engines is an important objective for automotive manufacturers, since stringent criteria for exhaust emissions must be met. In particular, (cold) starting is of exceptional importance owing to its significant contribution to the overall emissions during a transient test cycle. In the present work, experimental tests were conducted on a turbocharged and after-cooled bus-truck diesel engine in order to investigate the engine operating behaviour and the formation mechanisms of nitric oxide, smoke, and combustion noise during cold, warm, and hot starting. With this as a target, a fully instrumented test bed was set up, using ultra-fast response analysers capable of capturing the instantaneous development of emissions and various key engine and turbocharger parameters. The experimental test pattern included a variety of starting conditions, defined by the thermal status of the engine (i.e. the coolant temperature) and its idling speed. As expected, turbocharger lag was found to be the major contributor for the pollutant emissions spikes in all cases, with the thermal status of the engine and its idling speed playing important roles in the combustion (in)stability, turbocharger response, and noise radiation.

Keywords: turbocharged diesel engine, starting, transient emissions, nitric oxide, smoke opacity, combustion noise

1 INTRODUCTION

The turbocharged diesel engine is currently the preferred powertrain system in medium- and large-unit applications (trucks, land traction, ship propulsion, electricity generation, etc.). Moreover, it continuously increases its share in the highly competitive automotive market, having already ensured a market share comparable with that of the gasoline engine [1]. Owing to their overall superior efficiency, diesel-engined vehicles achieve much lower

fuel consumption and carbon dioxide emissions than their similarly rated spark ignition counterparts over the entire engine or vehicle operating range and lifetime.

So far, the study of diesel engine operation has primarily focused on the steady state performance. However, the majority of daily driving schedule involves transient conditions where only a very small portion of a vehicle's operating pattern is truly steady state, e.g. when cruising on a motorway. Consequently, the investigation of diesel engine transient operation has become an important objective to engine manufacturers, intensified by the fact that significant deviations are experienced when comparing instantaneous transient emissions with their quasi-steady counterparts [2–7]. Recognizing the above-mentioned findings, various legislative directives in the European Union, Japan,

*Corresponding author: Internal Combustion Engines Laboratory, Thermal Engineering Department, School of Mechanical Engineering, National Technical University of Athens, 9 Heron Polytechniou Street, Zografou Campus, 15780 Athens, Greece.
email: cdrakops@central.ntua.gr

and USA have drawn the attention of manufacturers and researchers to the transient operation of diesel engines in the form of Transient Cycles Certification for new vehicles [8, 9].

A case of diesel engine transient operation, which is special and very important in terms of combustion stability and emissions, is starting. Starting is distinguished as either cold or hot depending on the respective coolant (and oil) temperature. The former case has initiated much more vigorous research (see, for example, references [10] to [18]) owing to the significantly greater discrepancies experienced by the engine until it manages to reach a self-sustained rotational speed, compared with the relatively 'easier' case of hot starting [15–18].

In vehicular applications, starting is initiated and supported by the electric starter whereas, in larger-scale applications (marine and industrial), other methods are used (e.g. compressed air). Only the former case is considered in the current work (vehicular engine starting), since the engine under investigation is of an automotive type.

During the first few cycles (cranking phase) of a cold-starting event, the engine accelerates rapidly with the assistance of the electric starter. Subsequently, the engine speed continues to increase without the need for external assistance, until the point where stabilization to the idling speed is achieved. Increased amounts of soot (for turbocharged engines only), hydrocarbons, and carbon monoxide are expected during the cold-start phase, particularly if misfiring occurs, which is more likely the colder the ambient conditions. Misfiring is the most critical problem encountered during cold starting, which diversifies completely the response pattern from the other two major transient cases (load acceptance and acceleration), ultimately leading to combustion instability or even complete failure. Under misfiring conditions, which are influenced by a variety of factors, combustion cannot supply sufficient power to drive the engine and to overcome the increased friction losses; the latter emanate from the high lubricant viscosity at the low temperature. The intriguing fact is that, unlike acceleration or load acceptance, during cold starting, naturally aspirated engines suffer equally to their turbocharged counterparts [2].

As far as emissions are concerned, exhaust gases during cold starting have recently gained increased attention owing to their significant contribution to the total emissions from diesel-engined vehicles. For example, it has been found that a diesel engine may emit up to seven times more particulate matter during cold operation than under warm conditions

[15, 19] coupled also to a prolonged period of unacceptable smoke emissions [20]. The importance of cold-starting emissions has been further documented by the legislative transient cycles, e.g. the New European Driving Cycle or the US FTP-75, where the emissions have been, for some years now, sampled with the engine cold started.

The target of the current work is to expand past research on transient vehicular diesel engine operation under starting conditions and to shed more light on the relevant complex phenomena and underlying mechanisms, with the main focus being on the combustion development and emissions formation. With this target in mind, an extended set of tests was carried out on a turbocharged and after-cooled direct-injection bus-truck diesel engine. It is noted here that the majority of the research on starting has been conducted so far on an experimental basis (see, for example, references [15] to [20]) and mainly for naturally aspirated engines, whereas only a few simulation studies exist [21, 22]; it is not surprising that none of these includes emissions calculations.

The experimental schedule in this study included a plethora of starting tests under different coolant temperatures (the engine thermal status being 'cold', 'warm', or 'hot', i.e. fully warmed up) and idling speeds. The investigation carried out focused on combustion stability issues and on the two most influential diesel engine pollutants, namely nitric oxide (NO) and smoke (in terms of opacity), using ultra-fast response analysers particularly suited to transient experimentation. Moreover, the study was extended to another important, but often neglected, emission, namely combustion noise. Diesel engine noise radiation is attracting more and more attention in recent years [23, 24], since it is associated with the discomfort of passengers and pedestrians. The primary sources of noise generation in a diesel engine are gas flow (exhaust system), mechanical processes (e.g. valve train and gears), and combustion. The first source is substantially limited using mufflers (silencers) along the exhaust pipe. On the other hand, combustion noise prevails over other, mechanically originated noise radiation [2], and this is why only this source of noise was included in the current investigation.

2 DESCRIPTION OF THE EXPERIMENTAL INSTALLATION AND PROCEDURE

A general layout of the test bed installation, the instrumentation used, and the data acquisition system is illustrated in Fig. 1. A brief description of

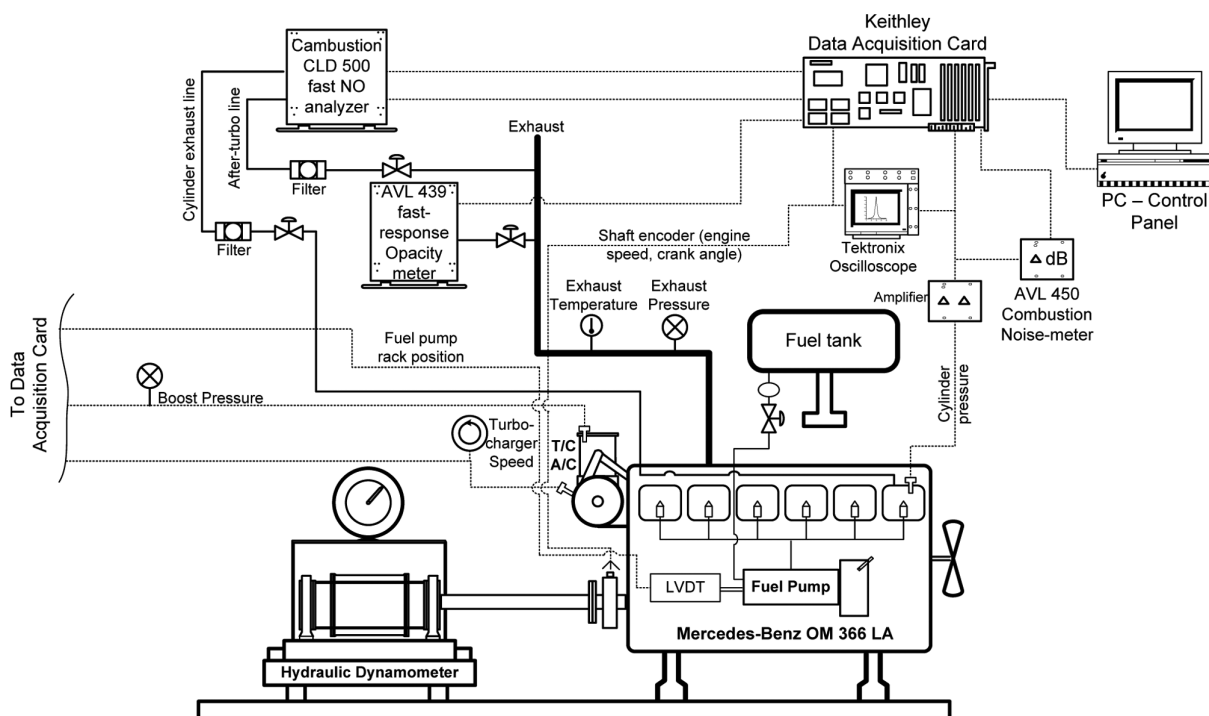


Fig. 1 Schematic arrangement of the test bed installation, instrumentation, and data acquisition system

the individual components will be given in the following sections. More details can be found in references [7] and [16].

2.1 Engine configuration and data acquisition system

The engine used in the current study is a Mercedes-Benz OM 366 LA, turbocharged and after-cooled, direct-injection diesel engine, following the Euro II emissions standard. It is widely used to power mini-buses and small-medium trucks. Its basic technical characteristics are given in Table 1. Two notable features of the engine are, on the one hand, its retarded fuel injection timing in order to achieve low NO emissions and, on the other hand, the fuel-limiter (cut-off) function (pneumatic control device) in order to limit the exhaust smoke level during demanding conditions such as transients or low-speed high-load steady state operation.

The engine and turbocharger operating parameters measured and recorded continuously were as follows: engine speed; cylinder pressure; fuel pump rack position; boost pressure; turbocharger speed. Table 2 provides a brief list of the various measuring devices used together with their measuring errors. The location of each of these on the experimental test bed installation is demonstrated in Fig. 1.

Table 1 Engine and turbocharger specifications

Engine model and type	Mercedes-Benz OM 366 LA six-cylinder, in-line, four-stroke compression ignition, direct-injection, water-cooled, turbocharged, and after-cooled, engine with bowl in piston
Emissions standard	Euro II
Speed range	800–2600 r/min
Maximum power	177 kW at 2600 r/min
Maximum torque	840 N m at 1250–1500 r/min
Engine total displacement	5958 cm ³
Bore	97.5 mm
Stroke	133 mm
Compression ratio	18:1
Fuel pump	Bosch PE-S series in-line, six-cylinder pump with fuel limiter
Static injection timing	5 ± 1° crank angle (CA) before top dead centre (at full load)
Turbocharger model	Garrett TBP 418-1 with internal wastegate
After-cooler	Air-to-air

Exhaust pressures and temperatures at various locations were also measured at steady state conditions after starting (idling) with conventional analogue devices. Additionally, fuel consumption measurements were undertaken during idling with the use of a gravimetric fuel tank. Finally, the engine coolant temperature and lubricating oil

Table 2 Measuring devices for the engine and turbocharger operating parameters

Parameter	Measuring device	Error
Engine speed	Kistler shaft encoder	0.02° CA
Cylinder pressure	Kistler miniature piezoelectric transducer, combined with Kistler charge amplifier	< ±1% full-scale output
Fuel pump rack position	Linear variable-differential transducer (LVDT)	0.1 mm
Boost pressure	Wika pressure transmitter	< ±1% full-scale output
Turbocharger speed	Garrett turbo speed sensor (including gauge)	± 0.5% full-scale output

pressure at idling conditions were provided through the engine instruments panel.

All the signals from the measuring devices and instruments were fed to the input of the data acquisition module, which is a Keithley KUSB 3102 ADC card connected to a Pentium dual-core personal computer via a USB interface. The specific card has a maximum sampling rate of 100 ksamples/s, with a 12 bit resolution for its eight differential analogue input channels. Following the storage of the recorded measurements into files, the data were processed using an in-house-developed computed code.

2.2 Emissions measurement

The emissions measured in this study were the two major pollutants from diesel engines, namely nitric oxide (NO) and smoke (in terms of opacity), as well as combustion noise.

NO was measured using the CLD500 gas analyser by Cambustion Ltd. This is a detector used for measuring the concentrations of NO and nitrogen oxides (NO_x) in the exhaust gas with a 90–10 per cent response time of approximately 2 ms for NO and 10 ms for NO_x [25]. Its operating principle is based on chemiluminescence, according to which the reaction between NO and ozone (O₃) emits light with intensity proportional to the NO concentration. The linearity of the analyser is within ±1 per cent full-scale output (FSO) and its drift less than ±1 per cent FSO per hour. The CLD500 has two remote sampling heads and it is capable of simultaneous sampling at two different locations. In the current test bed installation, the first head is located exactly after the exhaust valve of cylinder 1, and the second head is located downstream of the turbocharger, as shown in Fig. 1. For the current study, only the second sampling head was applied.

Exhaust gas (smoke) opacity was measured continuously with the AVL 439 partial flow opacimeter, which is particularly suitable for dynamic testing measurements with a response time less than 0.1 s and an accuracy of 0.1 per cent opacity. The opacimeter's technical characteristics comply with legal requirements such as ECE R24, SAE J 1667, and the European Load Response Test Cycle, with the

respective filter algorithms already preprogrammed [26]. In this study, no filter algorithm was applied ('raw' signal) in order to capture successfully all the smoke emission peaks. The location of the sampling and return lines is downstream of the turbocharger (Fig. 1).

Finally, combustion noise was measured with an AVL 450 combustion noise meter. Its operating principle is based on the analysis of the cylinder pressure in the frequency domain, by applying a series of filters to it, such as a U-filter, selectable low-pass filters, and an A-filter [27]. The origin of combustion noise in a diesel engine (the characteristic diesel combustion 'knock') lies in the high rate of cylinder pressure rise $dp/d\phi$, mainly during the premixed phase of combustion after the ignition delay. The total error of the device is less than ±1 dB. In the present work, the combustion noise meter was placed after the cylinder pressure signal amplifier (Fig. 1) and was operated without any low-pass filters.

2.3 Experimental procedure

The experimental schedule included a variety of starting tests at different idling speeds under cold, warm, and hot conditions, i.e. at different engine coolant and lubricating-oil temperatures. The detailed conditions of each test are summarized in Table 3; the lubricating-oil pressure is given only as an index of its temperature (the cooler the oil, the higher its pressure, for a constant engine idling speed). For each test, the pedal was fixed to a specific position corresponding to the desired engine idling speed and then the starter button was initiated. Overall, four idling speeds and four coolant temperatures were tried, as detailed in Table 3.

It must be highlighted that a preconditioning procedure was followed before most of the tests, in order to remove the deposited particulate matter on the exhaust pipe walls, which could be blown out and released during the following experimental trials [28]. This procedure was followed before the cold-starting (the day before the test) and the hot-starting (fully warmed-up) tests. It could not, however, be applied between the warm-starting cases,

Table 3 Summary of the test conditions

Test	Conditions	Idling speed (r/min)	Coolant temperature (°C)	Lubricating-oil pressure (bar)
1	Cold	900	20	5.9
2	Warm	1010	35	5.2
3	Warm	1010	60	4.0
4	Hot	1215	80	2.5
5	Hot	950	80	1.8

since it would cause a further warm-up of the engine, as it consists of engine operation at a high speed and a high temperature (load).

3 RESULTS AND DISCUSSION

3.1 Cold conditions: test 1

The first case of starting (test 1) was performed under cold conditions, i.e. the coolant and lubricating-oil temperatures were equal to ambient (20 °C for the present study). The development of various engine and turbocharger operating parameters and emissions for this test are illustrated in Fig. 2.

Before the engine was started, the fuel pump rack was located at its minimum position, as can be seen in Fig. 2. As soon as the starting event was initiated, the governor sensed the very low cranking speed (much lower than the required self-sustained speed) and forced the fuel pump rack to shift instantly to its maximum fuelling position. The initial sharp increase in the engine speed noticed in Fig. 2 for the first three cycles (lower left curve) was supported by the assistance of the electric starter. After the disengagement of the starter (cycle 3 or 1.4 s), the engine accelerated at a much slower rate. During this period, since there was clearly a lack of sufficient airflow due to the low engine and turbocharger rotational speeds, locally high fuel-to-air ratios were experienced, leading to flame quenching (owing to oxygen shortage) and combustion deterioration; the latter has been identified as responsible for combustion instability phenomena between consecutive cycles [10]. As the engine speed gradually increased, the rack moved progressively to a lower fuel supply position until it ultimately assumed its final steady state position after the engine had reached its idling self-sustained speed. It is very important to note here that, even after the engine speed had stabilized, the whole phenomenon continued to develop from the thermal point of view (thermal transient), since a much longer duration is required for the stabilization of exhaust gas, coolant, and lubricating-oil temperatures, as well as

for their cylinder and exhaust manifold wall counterparts owing to their high thermal inertia [2]. This thermal transient lasts for at least a few minutes, which is a relatively long period compared with the duration of the starting event (i.e. the time needed for the engine speed to stabilize to its idle value, which is of the order of a few seconds).

There are two remarks concerning engine and turbocharger operation in Fig. 2 that are worth discussing. The first is the combustion instability, documented by the highly unstable maximum cylinder pressure traces. For a more thorough understanding, a detailed view of the respective pressure diagrams during the first 16 engine cycles is provided in Fig. 3. Indeed, the cylinder pressure traces exhibit a high degree of variation from cycle to cycle (maximum deviation around 40 bar, excluding the first engine cycle), owing to incomplete combustion and occasionally leading to misfire. Owing to the low wall temperature during cold starting, the air charge in the cylinder may not reach temperatures capable of vaporizing the injected fuel. Consequently, formation of a combustible air–fuel mixture may be prohibited, ultimately leading to combustion instability (maybe also to complete combustion failure, but for much lower ambient temperatures than that during this study) with the engine compression ratio and starting aid playing primary roles. A key parameter is also the low injection pressure encountered at the low cranking speed that leads to poor spray penetration, atomization, and fuel evaporation [2]. Moreover, the synergistic effect of the low coolant temperature, which results in aggravated heat loss to the walls, the low lubricating-oil temperature, which causes higher frictional losses, and the low engine rotational speed, which allows more time for the above-mentioned two losses to develop and increases blow-by losses past the piston rings, all give rise to low compression pressures [29], leading eventually to the instability observed in Fig. 3.

The second notable finding during the cold-start test is the inlet manifold (boost) pressure drop during the first cycles, demonstrated in Fig. 2; this is related to the turbocharger lag. As can be further

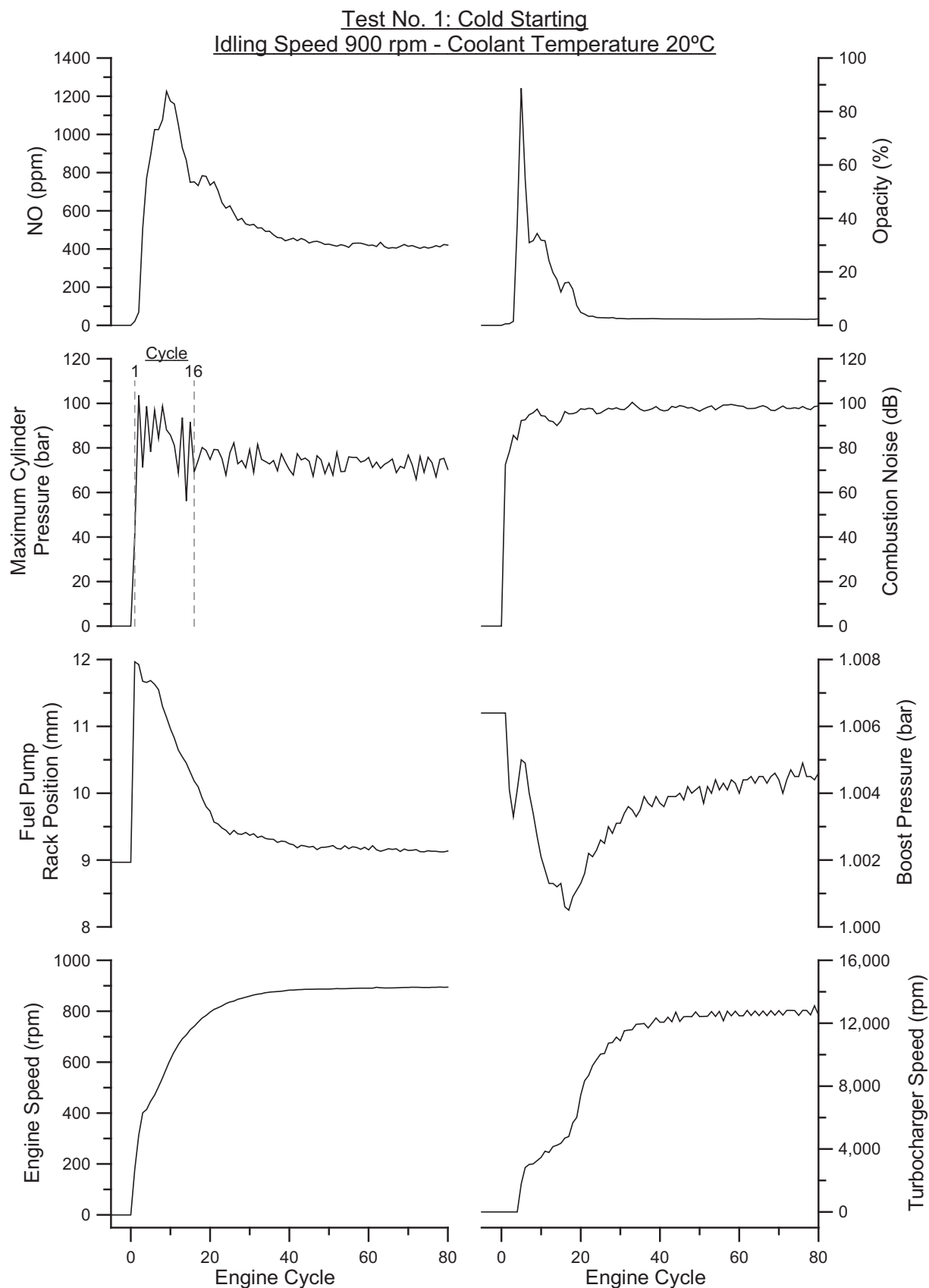


Fig. 2 Development of the engine and turbocharger variables and the emissions response during cold starting (test 1)

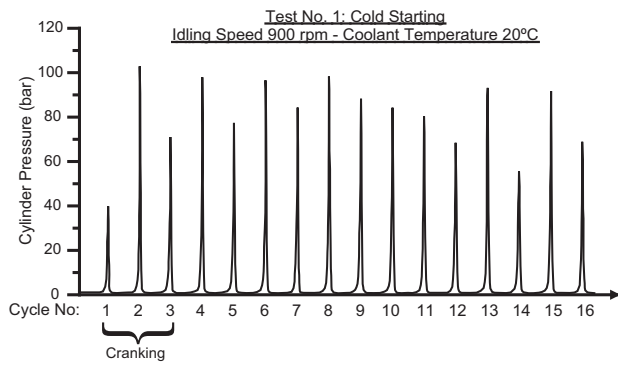


Fig. 3 Combustion instability during cold starting (test 1)

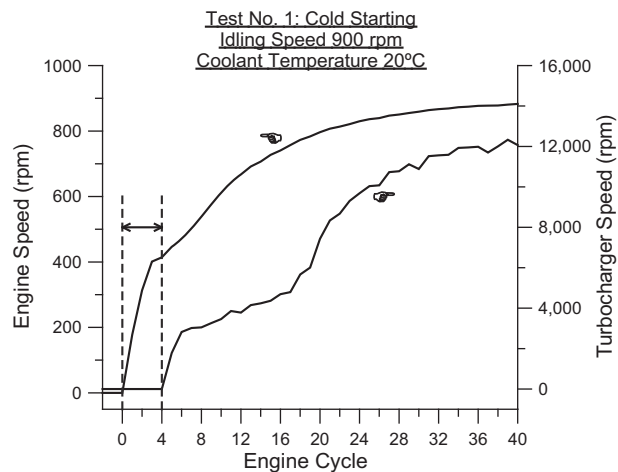


Fig. 4 Closer view of the engine and turbocharger speed developments during the first few cycles of cold starting (test 1)

observed in Fig. 4, during the first four cycles after initiation of the starter motor, the turbocharger compressor is not yet rotating (lower right curve in Fig. 2), while the engine is cranking. Hence, the engine sucks the available air in the inlet manifold, causing the drop in the boost pressure. Even after the turbocharger starts to accelerate, it can reach only relatively low rotational speeds and hence boost (since the latter is strongly dependent on turbocharger speed for aerodynamic-type compressors), owing to the poor energy content of the exhaust gas, which primarily originates in the high heat loss to the cold cylinder and exhaust manifold walls. As stated earlier, even after the engine speed has stabilized, the whole phenomenon continues to develop from the thermal point of view. This is explicitly demonstrated by the ongoing boost pressure development depicted in Fig. 5. The gradual heating of the cylinder and exhaust manifold walls leads to a decrease in the respective heat loss from the exhaust gases, increasing accordingly the

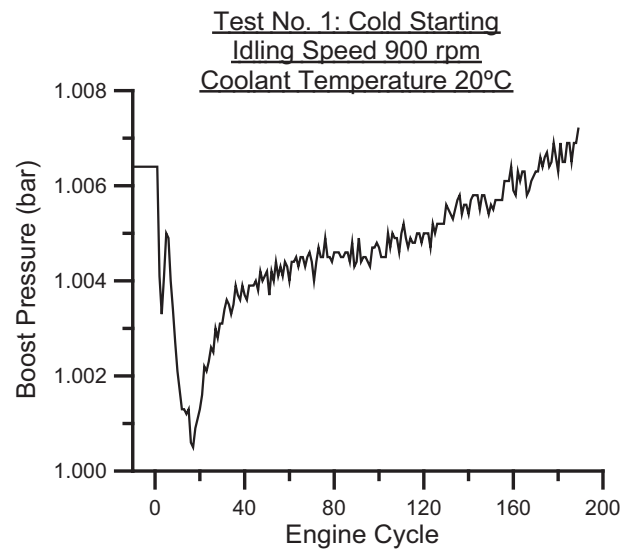


Fig. 5 Boost pressure development during cold starting (test 1)

available gas enthalpy at the turbine entry, and hence accelerating the turbocharger, which in turn produces a higher boost pressure.

The above-mentioned phenomena have also a direct impact on the pollutants emissions (mainly) and combustion noise radiation. Excessive black smoke is emitted from the exhaust pipe, identified by the extremely high values of exhaust gas opacity; the latter instantaneously assumes a value of near 100 percent as shown in the upper right curve in Fig. 2. The combination of high fuelling during cranking with the almost atmospheric inlet manifold pressure, resulting in very high fuel-to-air equivalence ratios, as well as the increased wall wetting from the fuel spray, are the evident reasons. As soon as combustion becomes stable (after almost 30 engine cycles or 6.2 s) and the engine speed reaches (or exceeds) its governing self-sustained speed, the rack moves towards the direction of reduced fuelling, with a subsequent decrease in the smoke emission. The latter is well known to be strongly influenced by the coolant temperature. The lower the ambient and/or coolant temperatures, the higher is the heat loss to the cylinder walls, resulting in a lower charge temperature, a longer ignition delay, and a more prolonged period of increased smoke emissions until the engine is fully warmed up [2]. It is noted here that the preconditioning procedure that was followed the day before the cold-starting test, as analysed previously, ensured that the smoke emission observed during this test consisted of soot particles produced only during the cold-starting event, and did not include any particles deposited on the exhaust pipe walls.

As regards NO emission, this again exhibits its peak value during the first cranking cycles. Nonetheless, this peak is experienced after the smoke opacity peak, and while the starter motor has been disengaged. After reaching its peak value, the NO emission trace is gradually reduced to its final value, but not for several engine cycles, however, owing to the slow development of the thermal transient events discussed earlier.

It is a common belief that, owing to the low gas temperatures involved during cold starting, NO emission is, in general, of secondary importance. In order to analyse the NO trend (upper left curve in Fig. 2), the contributions of various parameters have to be taken into account. On the one hand, first, the increased heat loss to the cylinder walls, resulting in low gas temperatures and, second, the very low boost pressures, which result in low oxygen availability, do not favour NO formation inside the cylinder. On the other hand, first, the increase in the ignition delay period combined with injection timing alteration due to the very low engine speed and, second, the high values of the fuel-to-air equivalence ratio, which locally reach stoichiometry, are well known to promote NO production.

Past research has shown that the longer ignition delay period, originating in the lower temperatures and pressures in the combustion chamber during cold starting, causes high rates of heat release at the initial stage of combustion, i.e. a more intense premixed combustion phase takes place [2, 10]. Hence, the production of NO may be actually favoured owing to *locally* high temperatures [18], although the *mean* temperature level is much below that during fully warmed-up conditions. Moreover, under certain circumstances, the latter mechanism might become dominant, causing an increasing trend of NO emission with lowering (ambient) temperature [18, 30].

In any case, for the results illustrated in Fig. 2, a very important factor determining their values is the units used for the quantification of NO. The volumetric concentration (ppm) assumes higher values the lower the engine rotational speed (and may thus lead to erroneous interpretations [31]) because the air mass is not suitably integrated with the ppm values. Furthermore, during cold starting, the air supply is low because of the very low boost pressure and turbocharger speed, resulting in high concentration values when the mass of NO is reduced to the total exhaust gas mass, as is the case in the present study.

The final class of emission studied is combustion noise, which is closely related to the cylinder

pressure [32] (Fig. 2). In fact, its measuring principle is based on processing of the measured indicator diagrams. Combustion noise (or, otherwise stated, combustion roughness) is determined primarily by the cylinder pressure rise rate (i.e. its gradient with respect to the CA) [33] during the engine cycle. This rate is influenced by a variety of parameters, including the injection timing and the ignition delay. Under cold-starting conditions, both these parameters behave differently compared with the fully warmed-up engine operation. In particular, the ignition delay effect is most influential; the low temperatures in the combustion chamber prevent fast fuel ignition, leading to a more intense premixed combustion phase, hence, steeper cylinder pressure gradients, and, consequently, higher combustion noise levels are experienced. As can be observed in Figs 2 and 3, combustion noise assumes a somewhat lower value at cycle 14 where misfire occurred (the latter can be documented by the respective very low maximum cylinder pressure).

3.2 Warm conditions: tests 2 and 3

The next two tests of the experimental schedule were conducted during the warm-up phase of the engine. Two intermediate coolant temperatures, namely 35 °C and 60 °C, were selected; the lubricating-oil temperature was affected accordingly, as indicated by its pressure in Table 3 (the cooler the oil, the higher is its pressure). Additionally, the cylinder and the exhaust manifold walls were hotter than with the cold-starting operation. The engine was shut down as soon as the coolant reached the desired temperature of each test and it was started immediately after. The (acceleration) pedal was kept at a constant position in order to ensure repeatability of the test and comparability of the two tests. In order to obtain a better insight into the engine behaviour during the test cases investigated here, a brief description of the shutdown process (preceding the starting) will be first presented.

An engine shutdown event is illustrated in Fig. 6. Here, only the qualitative profiles of engine speed and fuel pump rack position are important, since the focus is on the sequence of events and not on the absolute values. The engine was left to idle for several cycles before pulling manually the pedal in order to cut the fuel supply. In cycle 34, the engine speed started to fall because the fuel pump rack shifted backwards. Initially, the engine speed decreased gradually for about 35 cycles and then it fell sharply, after cycle 60, until the engine shut down. It is important to note here that the specific

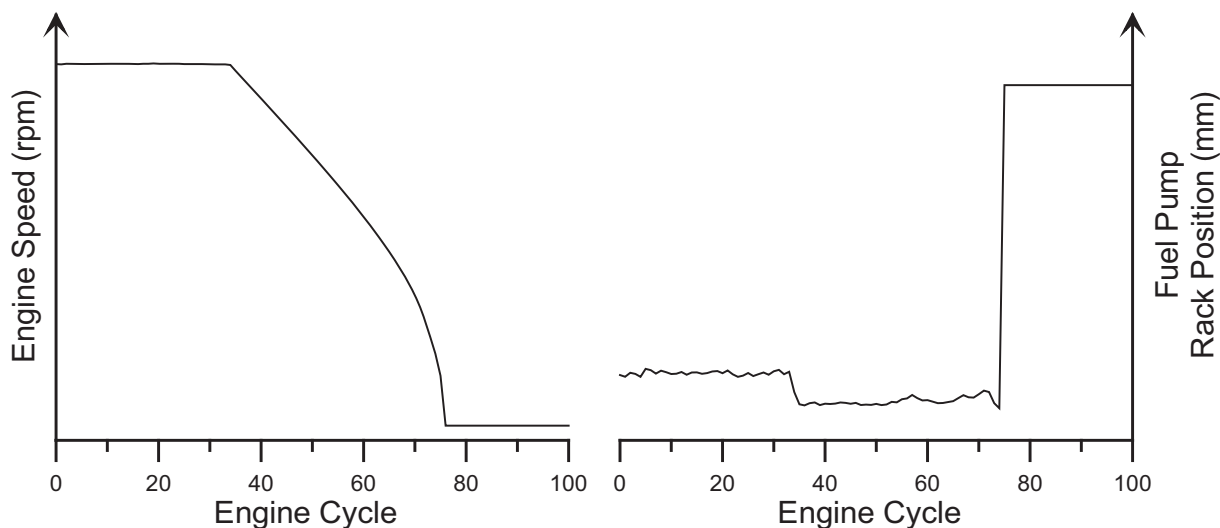


Fig. 6 Qualitative engine speed and fuel pump rack response during engine shutdown

speed profile is valid only for the current engine–hydraulic brake configuration; the latter plays an important role in the decrease in the rotating speed during shutdown, whereas other configurations may give different speed profiles. The governor responded to the abrupt speed drop by shifting the fuel pump rack to its maximum position (cycle 75 in the right-hand curve in Fig. 6); the latter, and this is very influential for the results that follow, stayed in this maximum position even after the engine operation had seized.

Immediately after shutdown, the starter button was initiated in order to restart the engine for the warm-starting tests. The development of the various engine and turbocharger operating parameters and emissions for the test cases examined are presented in Fig. 7. Although the final idling speed is slightly different from that of the cold-starting case discussed previously, most of the results are still comparable.

The first interesting point, independent of the engine idling speed, is the (qualitative) behaviour of the fuel pump rack. Contrary to the cold-starting case (Fig. 2), in the current test (Fig. 7), the rack was already in its maximum position at the instance that the engine started to rotate. However, it is not the starting conditions (in terms of the coolant temperature) that caused the different rack response, but the fact that for these tests the engine was started immediately after shutdown.

The second intriguing remark concerns the turbocharger response (lower right curves in Fig. 7). Compared with the cold-starting case of Fig. 2, the initial pressure drop is now much smaller. The turbocharger lag is less prominent here, owing to the higher energy content of the exhaust gas,

originating in the lower heat loss to the (now) warm cylinder and exhaust manifold walls. As a result, the turbocharger accelerates much more quickly, reaching higher rotational speeds. The significant impact that the thermal status of the engine has, during starting, on the turbocharger behaviour can be further revealed by comparing tests 2 and 3 with each other. Increasing the coolant temperature from 35 °C (test 2) to 60 °C (test 3) resulted in even faster turbocharger acceleration, concluding also in approximately 17 per cent higher final turbocharger speed.

As far as emissions are concerned, differences are again observed in comparison with the cold-start case analysed in the previous section, mainly as regards the absolute peak values and the duration of increased emissions. Beginning with smoke, the opacity reaches extremely high values during both test 2 and test 3, as can be seen in the upper right curve in Fig. 7 and in Fig. 8; these peak values, although lower, are in general comparable with those experienced during cold starting (Fig. 2). However, the high-smoke period is shorter than with test 1. For example, during test 1, the smoke opacity exceeded the 10 per cent value for 16 engine cycles (almost 3 s) while, for tests 2 and 3, the respective number of engine cycles is 12 during each case (2 s). Again, this behaviour is attributed to the turbocharger lag effect; the faster boost pressure evolution under warm conditions (originating in the faster turbocharger acceleration) offered higher oxygen availability, which in turn enhanced the oxidation of soot particles inside the cylinder and lowered the engine-out smoke.

Closer examination of the opacity development in Fig. 8 reveals higher peaks for test 3 than for test

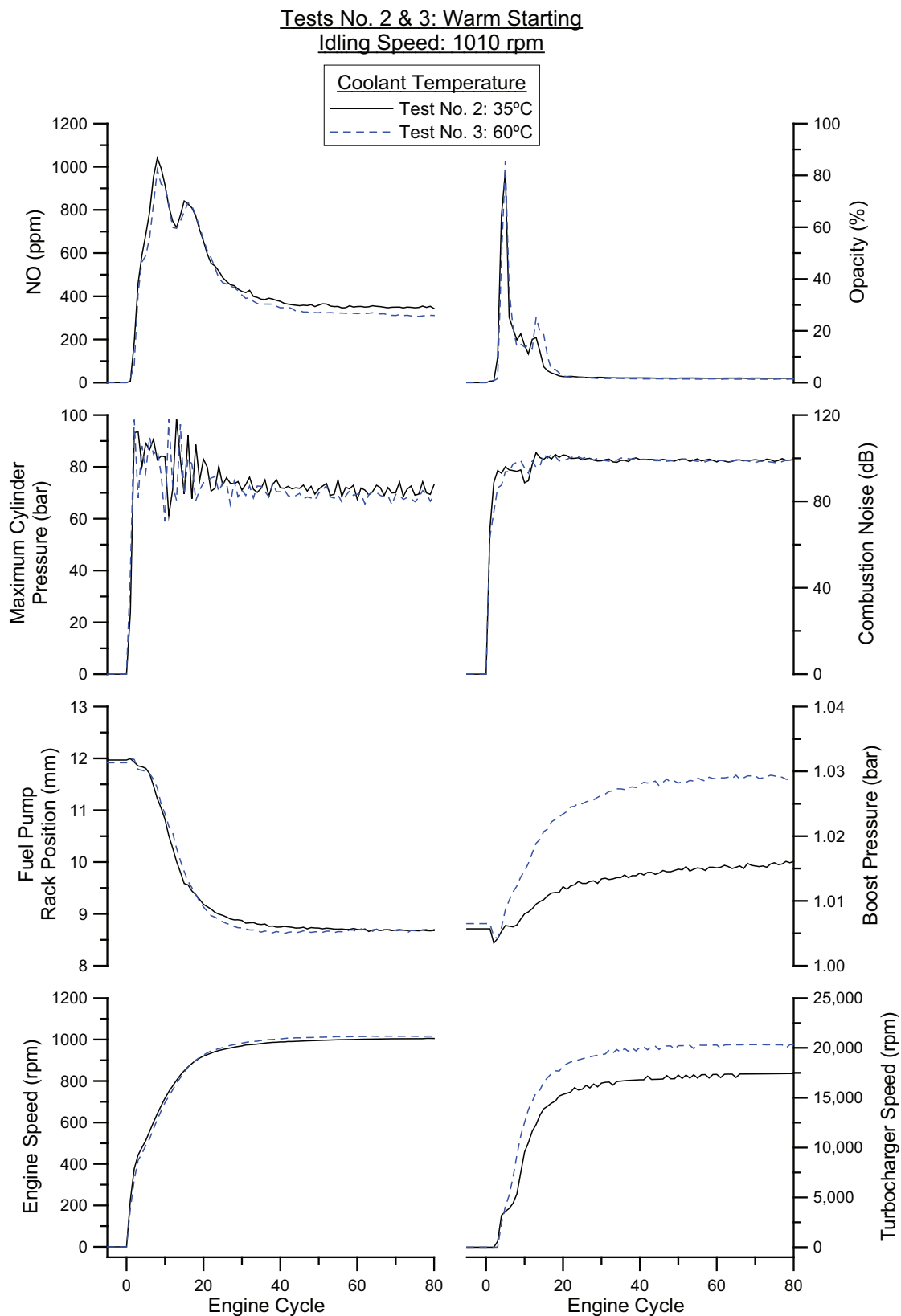


Fig. 7 Development of the engine and turbocharger variables and the emissions response during warm starting at two coolant temperatures (tests 2 and 3)

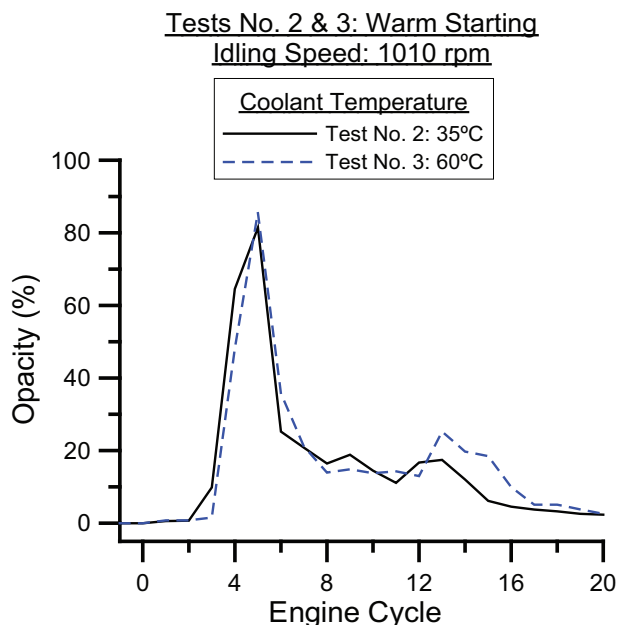


Fig. 8 Closer view of opacity development during the first few cycles of warm starting at two coolant temperatures (tests 2 and 3)

2, with the overall peaks being close to the respective peaks for test 1. The deposition of soot particles on the exhaust manifold pipe and their blow-out during the following starts should be taken into consideration in order to interpret these results. As explained in section 2, the engine preconditioning procedure could not be applied before each of the warm-starting tests. Thus, the smoke emission measurement unavoidably also includes a portion of the deposited soot particles, caused by the previous engine starts. It was impossible to separate these two sources of soot particles (in-cylinder formatted and exhaust manifold deposited). However, this measurement is actually closer to the real emissions experienced during daily driving.

Regarding NO emission, similar observations with the cold-starting case hold. A relatively high peak value is experienced for both test 2 and test 3 during the first cranking cycles, followed by a gradual reduction to the final value, as illustrated in the upper left curve in Fig. 7. Recall that this 'final' value does not remain constant owing to the development of the thermal transient mentioned previously. The overall NO concentration values are lower than those observed during cold starting, with the 'warmer' test 3 presenting slightly lower NO emission than the 'cooler' test 2. Again, the conflicting behaviour of all the previously discussed mechanisms influencing NO production should be taken into account, in order to interpret the results obtained.

The development of the third emission considered in this study, i.e. combustion noise, is also demonstrated in Fig. 7. A minimal variation in the combustion noise with the change in the coolant temperature is observed, mainly during the cranking cycles, with its values being of the same order of magnitude during both warm-starting tests. As mentioned previously, the change in the injection timing and the change in the ignition delay should be identified as the two influential parameters affecting combustion noise radiation. Injection timing plays an important role in the fuel spray development and air-fuel mixing, while the ignition delay becomes shorter (as the coolant temperature increases) owing to the smaller amount of heat lost from the gas to the warmer cylinder walls. All in all, it seems that the low cranking speed of the engine, which induces low cylinder pressure increase rates, has the dominant impact on combustion noise development during these starting tests.

3.3 Hot conditions: tests 4 and 5

The last two tests were performed under fully warmed-up (hot) conditions, at two idling speeds (see also Table 3). The accelerator pedal was set to the desired idling speed position and the engine was shut down; the starter button was immediately pressed to start the engine again. Before each hot-starting test, the preconditioning procedure was followed, as analysed in section 2. The development of various engine and turbocharger operating parameters and emissions for the test cases examined here is illustrated in Fig. 9.

The thermal status of the engine in the fully warmed-up conditions as well as its speed are the two contributing factors that determine the subsystems behaviour during these starting tests. In both cases, the fuel pump rack initiates exactly from the position reached during the preceding shutdowns (as discussed previously), gradually shifting backwards as the engine attains the governing self-sustained speed. For higher idling speeds, as in test 4, the rack remains longer in the maximum fuelling position, before stabilizing finally at a higher position. As in all previous cases, independently of the engine thermal status, the initial sharp engine speed increase (lower left curve in Fig. 9) is attributed to the electric starter action.

The starting conditions and the required idling speed affect the turbocharger response too; the latter accelerates more quickly than in all the previous tests, owing to the much higher exhaust gas energy content, originating in the (much) lower heat loss to the now fully warmed-up cylinder and

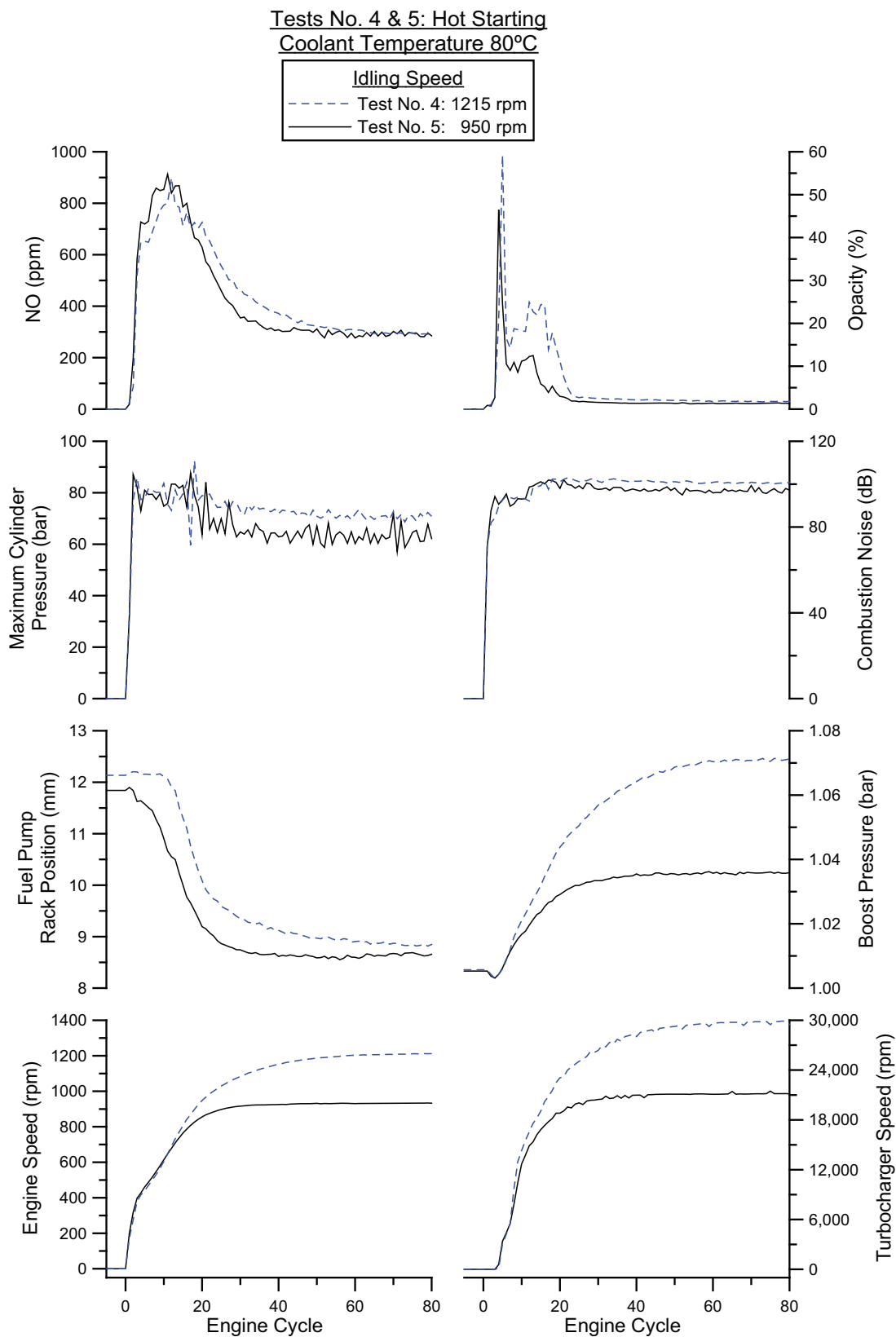


Fig. 9 Development of the engine and turbocharger variables and the emissions response during hot starting at two idling speeds (tests 4 and 5)

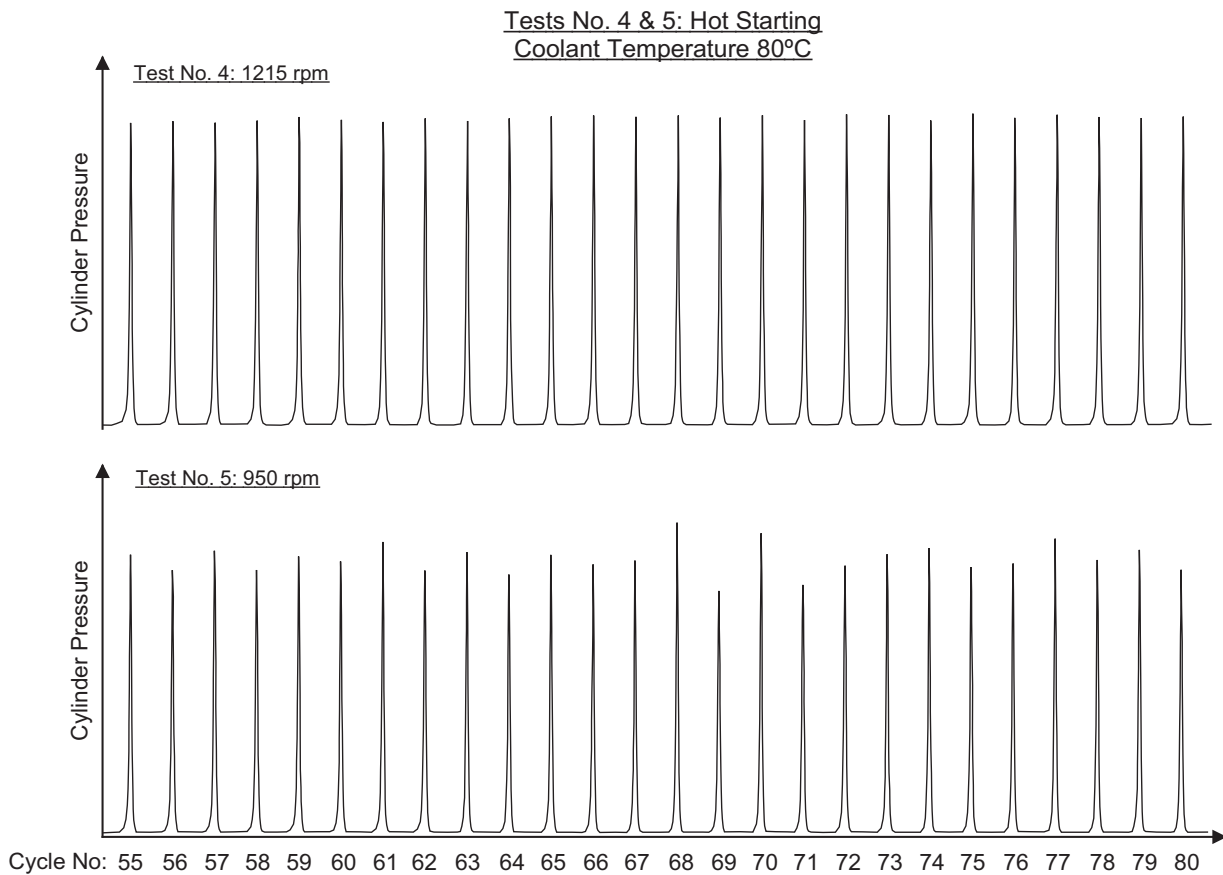


Fig. 10 Cylinder pressure diagrams during idling at two idling speeds during hot starting (tests 4 and 5)

exhaust manifold walls. This can be further supported by a direct comparison of the final turbocharger speed reached during tests 3 and 5. Although in the latter test, the engine idling speed is lower, the turbocharger reaches an almost 4 per cent higher rotational speed compared with the former test, which clearly arises because the hotter exhaust gas enters the turbine. As a result, the turbocharger lag is less decisive and the initial boost pressure drop smaller. Finally, and following engineering intuition, both the turbocharger speed and the compressor boost pressure assume higher values for the case of higher engine idling speed (test 4) compared with the lower idling speed of test 5.

Another interesting finding concerns the combustion behaviour during idling. After the engine speed has stabilized, combustion appears to be more stable during test 4; this is documented by the almost constant maximum cylinder pressure traces illustrated in Fig. 9. Closer examination of the cylinder pressure traces between engine cycles 55 and 80 is given in Fig. 10 and supports this observation. On the other hand, combustion presents instability

during test 5, as can also be documented in Fig. 10. The different engine idling speed is the evident reason for that behaviour. The higher engine speed of test 4 produces higher compression pressures, and thus temperatures, ensuring faster ignition, while the higher air supply promotes combustion. On the other hand, the lower idling engine speed of test 5 causes higher blow-by loss past the piston rings compared with the previous case and allows more time for the heat loss to develop, resulting eventually in the combustion instability observed in Fig. 10.

As regards emissions, the main focus is again on exhaust gas opacity. Smoke assumes very high values during both tests, as shown in Fig. 9, significantly lower, however, than for the previous (cold or warm) cases (less than 60 per cent in test 4 compared with 90 per cent in test 1). As the coolant temperature increases, the higher air supply (owing to the 'milder' turbocharger lag) prevents the formation of high fuel-to-air equivalence ratios inside the cylinder, while the higher in-cylinder temperatures (originating in the lower heat loss) promote soot oxidation. Moreover, the increased inlet air density,

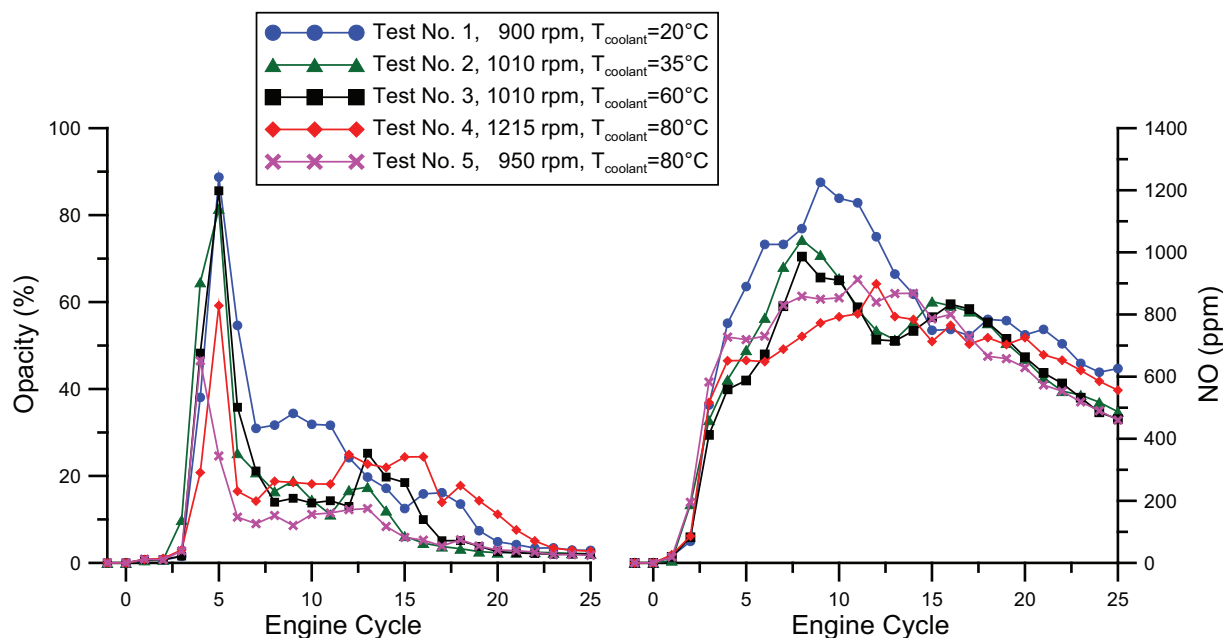


Fig. 11 Comparative soot and NO emissions development during cold-, warm- and hot-starting tests

resulting from the higher boost pressure, reduces the wall-wetting effect of the fuel spray after injection. Peak opacity values are again attributed to turbocharger lag, being prominent mainly during the cranking cycles. In the case of the higher engine idling speed, as in test 4, the peak opacity value is higher than for test 5, while the smoky period is also extended, as exhibited in Fig. 9. For example, during test 4 the smoke opacity exceeds 10 percent for 17 engine cycles (2.9 s), while in test 5 this happens for 'only' nine engine cycles (1.5 s). The reason for this behaviour is the greater fuel pump rack displacements for the case of the higher idling speed (Fig. 9, test 4). It must be noted here that the preconditioning procedure followed before tests 4 and 5, as described in section 2, ensures that the smoke emission observed in these cases consists of only soot particles produced in the cylinder and does not include any deposited particles on the exhaust pipe walls.

As far as NO emission is concerned (upper left curve in Fig. 9), similar values are experienced for both test 4 and test 5, overall lower, however, than their counterparts of the previous cases in Figs 2 and 7. Again, in order to explain this behaviour, all the parameters affecting NO formation should be taken into consideration. With increasing coolant temperature, the heat loss to the cylinder walls becomes smaller and more oxygen is available, thus promoting NO production, while the ignition delay is shorter (resulting in less intense premixed

combustion) and the mismatch between the fuel and the air supply is less extensive (weaker effect of turbocharger lag), being unfavourable for NO formation. The higher values of NO experienced during test 4 than in test 5 are attributed to the greater fuel pump rack displacements and the higher combustion pressures, as documented in Fig. 9.

Finally, combustion noise is notably affected by the idling engine speed, as illustrated in Fig. 9. In the case of a higher idling speed, combustion noise assumes higher values, owing to the steeper cylinder pressure increase. As in all previous cases, the variation in the injection timing and the variation in the ignition delay play important roles in the combustion noise development. Specifically, the ignition delay becomes shorter, the hotter the starting conditions, resulting in less intense premixed combustion. However, a direct comparison between the cold- and warm-starting cases is not feasible, because of the different idling speeds.

Concluding the discussion of the experimental findings, Figs 11 and 12 summarize the exhaust emissions results by illustrating the opacity and the NO development for all the starting cases studied (Fig. 11) as well as the peak values for each coolant temperature involved (Fig. 12). In all cases and for both exhaust pollutants, the same trend is experienced on a qualitative basis; a very high peak is initially experienced, followed by a gradual stabilization to a lower value (Fig. 11). The latter is not

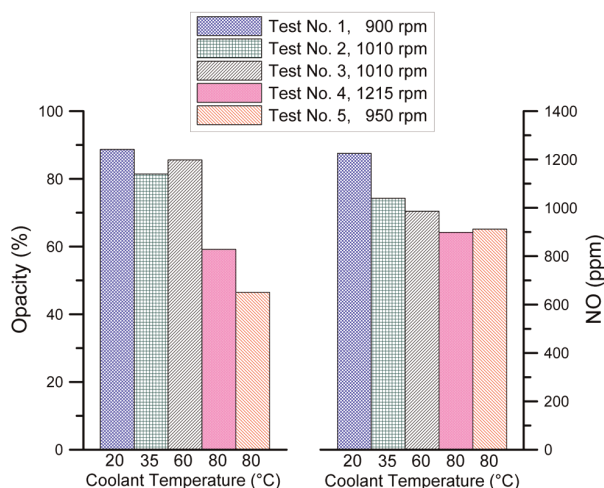


Fig. 12 Peak soot and NO emissions versus coolant temperature

constant but rather continues to develop (especially for NO emission) owing to the thermal transient effects, discussed earlier.

As regards Fig. 12, a decreasing trend of the maximum opacity value is observed with increasing coolant temperature, taking the engine idling speed also into account. The only exception is for test 3, where the peak opacity value exceeds the respective value for test 2, and this is attributed to the deposition of soot particles on the exhaust manifold, as detailed earlier.

4 SUMMARY AND CONCLUSIONS

A fully instrumented test bed installation has been set up in order to study the transient performance and emissions of an automotive turbocharged diesel engine during starting. Ultra-fast response analysers were employed to measure the NO concentration, smoke opacity, and combustion noise. A variety of starting tests was conducted at different idling speeds and coolant temperatures. The instantaneous emission results of the experimental investigation were discussed in conjunction with the engine and turbocharger response.

The basic conclusions derived from the current investigation and for the specific engine-brake configuration, are summarized as follows.

1. Turbocharger lag was found to be the most notable contributor for all starting discrepancies, and the major cause for peak pollutant emissions values.
2. Combustion instability and extremely high values of exhaust gas opacity were experienced mainly during cold starting.

3. The thermal status of the engine and its idling speed played important roles in the combustion stability and the turbocharger response. Specifically, as the engine got hotter and was operated at a higher idling speed, combustion became more stable, and the turbocharger accelerated more quickly, producing a higher boost pressure.
4. The low cranking speed of the engine during starting appeared to have the dominant effect on combustion noise development.
5. Higher idling speeds result in elevated exhaust gas opacity values and prolonged smoky period, combined with higher combustion noise levels.
6. A lowering trend in the NO peak value (ppm) was observed as the engine became hotter.

ACKNOWLEDGEMENTS

The authors would like to thank Cambustion Ltd (Cambridge, UK) for the loan of the CLD500 NO analyser and their continuous support during the experiments. Special thanks are due to Turbo Hellas Trading Ltd for the donation of the turbocharger speed sensor kit used in the experiments.

© Authors 2011

REFERENCES

- 1 ACEA European Automobile Manufacturers' Association, 2011, available from <http://www.acea.be>.
- 2 **Rakopoulos, C. D. and Giakoumis, E. G.** *Diesel engine transient operation*, 2009 (Springer, London).
- 3 **Hagena, J. R., Filipi, Z. S., and Assanis, D. N.** Transient diesel emissions: analysis of engine operation during a tip-in. SAE paper 2006-01-1151, 2006.
- 4 **Rakopoulos, C. D. and Giakoumis, E. G.** Review of thermodynamic diesel engine simulations under transient operating conditions. SAE paper 2006-01-0884, 2006.
- 5 **Gullett, B. K., Touati, A., Oudejans, L., and Ryan, S. P.** Real-time emissions characterisation of organic air toxic pollutants during steady-state and transient operation of a medium duty diesel engine. *Atmos. Environ.*, 2006, **40**, 4037–4047.
- 6 **Eastwood, P. G., Tufail, K., Winstanley, T., Darlington, A., Karagiorgis, S., Hardalupas, Y., and Taylor, A. M. K. P.** Estimation of deviations in NO and soot emissions between steady-state and EUDC transient operation of a common-rail diesel engine. SAE paper 2009-24-0147, 2009.
- 7 **Rakopoulos, C. D., Dimaratos, A. M., and Giakoumis, E. G.** Experimental study of transient nitric oxide, smoke and combustion noise emissions during acceleration of an automotive

- turbocharged diesel engine. *Proc. IMechE, Part D: J. Automobile Engineering*, 2011, **225**(2), 260–279.
- 8 European Commission, Enterprise and Industry, Automotive section: directives and regulations on motor vehicles, 2009, available from http://ec.europa.eu/enterprise/sectors/automotive/documents/directives/motor-vehicles.index_en.htm.
 - 9 United States Environmental Protection Agency, Testing and measuring emissions, 16 June 2010, available from <http://www.epa.gov/nvfel/testing/dynamometer.htm#engcycles>.
 - 10 Henein, N. A., Zahdeh, A. R., Yassine, M. K., and Bryzik, W. Diesel engine cold starting: combustion instability. SAE paper 920005, 1992.
 - 11 Engler, D., Hausberger, S., and Blassnegger, J. Cold start emissions of heavy duty vehicles. SAE paper 2001-24-0077, 2004.
 - 12 Cotte, H., Bessagnet, B., Blondeau, C., Mallet-Hubert, P.-Y., Momique, J.-C., Walter, C., Boulanger, L., Deléger, D., Jouvenot, G., Clarisse, P., and Rouveïrolles, P. Cold-start emissions from petrol and diesel vehicles according to the emissions regulations (from Euro 92 to Euro 2000). *Int. J. Veh. Des.*, 2001, **27**, 275–285.
 - 13 Osuka, I., Nishimura, M., Tanaka, Y., and Miyaki, M. Benefits of new fuel injection technology on cold startability of diesel engines – improvement of cold startability and white smoke reduction by means of multi injection with common rail fuel system (ECD-U2). SAE paper 940586, 1994.
 - 14 Peng, H.-Y., Cui, Y., Deng, K.-Y., Shi, L., and Li, L.-G. Combustion and emissions of a direct-injection diesel engine during cold start under different exhaust valve closing timing conditions. *Proc. IMechE, Part D: J. Automobile Engineering*, 2008, **222**(1), 119–129.
 - 15 Bielaczyc, P., Merkisz, J., and Pielecha, J. Investigation of exhaust emissions from DI diesel engine during cold and warm start. SAE paper 2001-01-1260, 2001.
 - 16 Rakopoulos, C. D., Dimaratos, A. M., Giakoumis, E. G., and Peckham, M. S. Experimental assessment of turbocharged diesel engine transient emissions during acceleration, load change and starting. SAE paper 2010-01-1287, 2010.
 - 17 Belardini, P., Bertoli, C., Del Giacomo, N., and Iorio, B. Combustion and pollutant emissions from light duty diesel engines: the influence of mixing process and transient operating conditions. *Sci. Total Environ.*, 1993, **134**, 285–293.
 - 18 Ogawa, H., Raihan, K. A., Ilizuka, K.-I., and Miyamoto, N. Cycle-to-cycle transient characteristics of diesel emissions during starting. SAE paper 1999-01-3495, 1999.
 - 19 Wachter, W. F. Analysis of transient emissions data of a model year 1991 heavy duty diesel engine. SAE paper 900443, 1990.
 - 20 Arcoumanis, C. and Yao, X. G. Transient smoke and unburnt hydrocarbon emissions during cold-start in a turbo-charged DI diesel engine. In *Proceedings of the IMechE Seminar on Transient performance of engines*, 1994, pp. 43–60, 1994 (Mechanical Engineering Publications Ltd, London).
 - 21 Liu, H.-Q., Chalhoub, N. G., and Henein, N. Simulation of a single cylinder diesel engine under cold start conditions using simulink. *Trans. ASME, J. Engng. Gas Turbines Power*, 2001, **123**, 117–124.
 - 22 Henry, R. R. An engine-starting simulation with friction estimation: background and model validation. In *Proceedings of the 2003 ASME International Mechanical Engineering Congress (IMECE'03)*, Washington, DC, USA, 15–21 November 2003, paper no. IMECE2003-43060.
 - 23 Dhaenens, M., Van der Linden, G., Nehl, J., and Thiele, R. Analysis of transient noise behaviour of a truck diesel engine. SAE paper 2001-01-1566, 2001.
 - 24 Commission Directive 96/20/EC of 27 March 1996 adapting to technical progress Council Directive 70/15/EEC relating to the permissible sound level and the exhaust system of motor vehicles. *Off. J.*, April 1996, L092.
 - 25 *CLD500 Fast NO_x measurement system, user manual (version 2.2)*, 2008 (Cambustion Ltd, Cambridge).
 - 26 *AVL 439 Opacimeter, operating manual*, November 2006 (AVL, Graz).
 - 27 *AVL 450 Combustion noise meter, operating manual*, August 2000 (AVL, Graz).
 - 28 Andrews, G. E., Clarke, A. G., Rojas, N. Y., Sale, T., and Gregory, D. The transient storage and blow-out of diesel particulate in practical exhaust systems. SAE paper 2001-01-0204, 2001.
 - 29 Cheng, K. Y., Shayler, P. J., and Murphy, M. The influence of blow-by on indicated work output from a diesel engine under cold start conditions. *Proc. IMechE, Part D: J. Automobile Engineering*, 2004, **218**(3), 333–340.
 - 30 Weilenmann, M., Favez, J.-Y., and Alvarez, R. Cold-start emissions of modern passenger cars at different low ambient temperatures and their evolution over vehicle legislation categories. *Atmos. Environ.*, 2009, **43**, 2419–2429.
 - 31 Grados, C. V. D., Uriondo, Z., Clemente, M., Espadafor, F. J. J., and Gutiérrez, J. M. Correcting injection pressure maladjustments to reduce NO_x emissions by marine diesel engines. *Transp. Res., Part D: Transp. Environ.*, 2009, **14**, 61–66.
 - 32 Taylor, C. F. *The internal combustion engine in theory and practice*, vol. 2, 1985 (MIT Press, Cambridge, Massachusetts).
 - 33 Osawa, H. and Nakada, T. Pseudo cylinder pressure excitation for analysing the noise characteristics of the engine structure. *JSAE Rev.*, 1999, **20**, 67–72.